12. Carroll, D. L. *et al.* Electronic structure and localized states at carbon nanotube tips. *Phys. Rev. Lett.* **78,** 2811–2814 (1997).
13. Dresselhaus, M. S. Dresselhaus, G. & Eklund, P. C. *Science of Fullerenes and Carbon Nanotubes* (Academic, San Diego, 1996).
14. Thess, A. *et al.* Crystalline ropes of metallic carbon nanotubes. *Science* **273,** 483–487 (1996).
15. Cowley, J. M., Nikolaev, P., Thess, A. & Smalley, R. E. Electron nano-diffraction study of carbon single-walled nanotube ropes. *Chem. Phys. Lett.* **265,** 379–384 (1997).
16. Venema, L. C. *et al.* STM atomic resolution images of single-wall carbon nanotubes. *Appl. Phys. A* (in the press).
17. Mintmire, J. W., Robertson, D. H. & White, C. T. Properties of fullerene nanotubules. *J. Phys. Chem. Solids* **54,** 1835–1840 (1993).
18. White, C. T. *et al.* in *Buckminsterfullerenes* (eds Billups, W. E. & Ciufolini, M. A.) 125–184 (VCH, Weinheim, 1993).
19. Kane, C. L. & Mele, E. J. Size, shape, and low energy electronic structure of carbon nanotubes. *Phys. Rev. Lett.* **78,** 1932–1936 (1997).
20. Gadzuk, J. W. Resonance-tunneling spectroscopy of atoms adsorbed on metal surfaces: theory. *Phys. Rev. B* **1,** 2110–2129 (1970).
21. Stroscio, J. A., Feenstra, R. M. & Fein, A. P. Electronic structure of the Si(111)2 × 1 surface by scanning tunneling spectroscopy. *Phys. Rev. Lett.* **57,** 2579–2582 (1986).
22. Feenstra, R. M., Stroscio, J. A. & Fein, A. P. Tunneling spectroscopy of the Si(111)2 × 1 surface. *Surf. Sci.* **181,** 295–306 (1987).
23. Lang, N. D. Spectroscopy of single atoms in the scanning tunneling microscope. *Phys. Rev. B* **34,** R5947–R5950 (1986).
24. Hamers, R. J. in *Scanning Tunneling Microscopy and Spectroscopy* (ed. Bonnell, D. A.) 51–103 (VCH, New York, 1993).
25. Wildöer, J. W. G., van Roij, A. J. A., van Kempen, H. & Harmans, C. J. P. M. Low-temperature scanning tunneling microscope for use on artificially fabricated nanostructures. *Rev. Sci. Instrum.* **65,** 2849–2852 (1994).

Acknowledgements. The first two authors contributed equally to the present work. We thank S. J. Tans and J. C. Charlier for discussions, and L. P. Kouwenhoven, J. E. Mooij and P. M. Dewilde for support. The work at Delft was supported by the Dutch Foundation for Fundamental Research of Matter (FOM). The nanotube research at Rice was funded in part by the US NSF, the Texas Advanced Technology Program and the Robert A. Welch Foundation.

Correspondence and requests for materials should be addressed to C.D. (e-mail: dekker@qt.tn.tudelft.nl).

Atomic structure and electronic properties of single-walled carbon nanotubes

Teri Wang Odom*, Jin-Lin Huang*, Philip Kim† & Charles M. Lieber*†

** Department of Chemistry and Chemical Biology, and † Division of Engineering and Applied Sciences, Harvard University, Cambridge, Massachusetts 02138, USA*

Carbon nanotubes[1] are predicted to be metallic or semiconducting depending on their diameter and the helicity of the arrangement of graphitic rings in their walls[2–5]. Scanning tunnelling microscopy (STM) offers the potential to probe this prediction, as it can resolve simultaneously both atomic structure and the electronic density of states. Previous STM studies of multi-walled nanotubes[6–9] and single-walled nanotubes (SWNTs)[10] have provided indications of differing structures and diameter-dependent electronic properties, but have not revealed any explicit relationship between structure and electronic properties. Here we report STM measurements of the atomic structure and electronic properties of SWNTs. We are able to resolve the hexagonal-ring structure of the walls, and show that the electronic properties do indeed depend on diameter and helicity. We find that the SWNT samples exhibit many different structures, with no one species dominating.

The diameter and helicity of a defect-free SWNT are uniquely characterized by the vector $\mathbf{c_h} = n\mathbf{a_1} + m\mathbf{a_2} \equiv (n, m)$ that connects crystallographically equivalent sites on a two-dimensional graphene sheet, where $\mathbf{a_1}$ and $\mathbf{a_2}$ are the graphene lattice vectors and n and m are integers (Fig. 1). Electronic band structure calculations[2–5] predict that the (n,m) indices determine the metallic or semiconducting behaviour of SWNTs. Zigzag $(n,0)$ SWNTs should have two distinct types of behaviour: the tubes will be metals when $n/3$ is an integer, and otherwise semiconductors[3–5]. As $\mathbf{c_h}$ rotates away from $(n,0)$, chiral (n,m) SWNTs are possible with electronic properties similar to the zigzag tubes; that is, when $(2n + m)/3$ is an integer the tubes are metallic, and otherwise semiconducting. The gaps of the semiconducting $(n,0)$ and (n,m) tubes should depend inversely on diameter. Finally, when $\mathbf{c_h}$ rotates 30° relative to $(n,0)$, $n = m$. The (n,n) or armchair tubes are expected to be truly metallic with band crossings at $\mathbf{k} = \pm 2/3$ of the one-dimensional Brillouin zone. It has been suggested that SWNT samples produced by laser vaporization[11] and arc[12] methods consist predominantly of (10,10) metallic armchair tubes.

We have carried out STM measurements in ultra-high vacuum at 77 K on purified SWNT samples produced by laser vaporization[11]. Typical atomically resolved images of a SWNT on the surface of a rope, which consists of parallel tubes[11], and isolated SWNTs on a Au(111) substrate are shown in Fig. 2a and b, respectively. Figure 2a shows the expected honeycombe lattice for a SWNT with a C–C spacing of 0.14 ± 0.02 nm. The chiral angle is readily determined by identifying the zigzag tube axis direction (the line connecting sites separated by 0.426 nm) relative to the sample tube axis. This shows quite clearly that the tube is chiral with an axis orientated at an angle of −8.0 ± 0.5° relative to that for a zigzag nanotube. As the tube axis is perpendicular to $\mathbf{c_h}$, this corresponds to the angle between $\mathbf{c_h}$ and $(n,0)$ in Fig. 1. From this angle and the measured diameter of 1.0 ± 0.05 nm, we can assign (n,m) indices of either (11,2) or (12,2); the angle/diameter for (11,2) and (12,2) are −8.2°/0.95 nm and −7.6°/1.03 nm, respectively. We note that an (11,2) tube is expected to be metallic, whereas a (12,2) tube should be semiconducting. The helicity of the lower isolated SWNT in Fig. 2b was determined in a similar manner, yielding a chiral angle of −11.0 ± 0.5°; the diameter of this tube is 1.08 ± 0.05 nm. These parameters match closely the values expected for a (12,3) tube, ±10.9°/1.08 nm, and reasonably exclude other choices of indices.

Central to the work reported here is our ability to characterize the electronic properties of the atomically resolved nanotubes by tunnelling spectroscopy. Specifically, current (I) versus voltage (V) was measured at specific sites along the tubes and differentiated to yield the normalized conductance, $(V/I)\mathrm{d}I/\mathrm{d}V$, which has been shown[13] to provide a good measure of the main features in the local density of electronic states (LDOS) for metals and semiconductors. The gradual increase in current in the I–V data (Fig. 2c, d) recorded on the SWNTs imaged in Fig. 2a, b shows qualitatively that both tubes are metallic. The LDOS determined from data sets recorded at different locations along the tubes are very similar, demonstrating the reproducibility of the measurements; furthermore, the LDOS for both tubes are roughly constant between −600 and +600 mV as expected for a metal. Small variations in the LDOS with energy are not significant and arise from noise in the data. These spectroscopy results are similar to those obtained on the Au(111) substrate except that the surface state 450 meV below the Fermi level[14] is also observed on the latter.

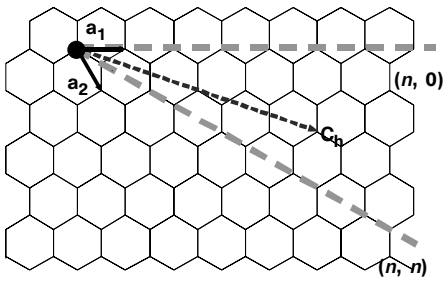

Figure 1 Schematic of a two-dimensional graphene sheet illustrating lattice vectors $\mathbf{a_1}$ and $\mathbf{a_2}$, and the roll-up vector $\mathbf{c_h} = n\mathbf{a_1} + m\mathbf{a_2}$. The limiting cases of $(n,0)$ zigzag and (n,n) armchair tubes are indicated with dashed lines. As represented here, the angle between the zigzag configuration and $\mathbf{c_h}$ is negative.

The metallic behaviour of our (12,3) tube is in agreement with the prediction that $(2n + m)/3$ is an integer, and additionally suggests that the indices for the tube in Fig. 2a are (11,2) rather than (12,2). We have also characterized a metallic, achiral zigzag SWNT with a diameter of 0.95 ± 0.05 nm. This diameter is very close to the expected 0.94 nm diameter of a (12,0) tube, although possibly indistinguishable from the 1.02 nm diameter expected for a (13,0) tube. There are two other important points that these data address. First, curvature in the graphene sheet of a SWNT should cause the π/σ bonding and π^*/σ^* antibonding orbitals on carbon to mix and create a small gap at the Fermi level in these metallic tubes[3,5]. We have not observed evidence for this small gap, although it is possible that the thermal energy at 77 K, 7 meV, smears the gap structure predicted to be of the order of 8 meV for a (12,0) tube[3]. Second, the LDOS recorded on metallic SWNTs in a rope and isolated on the substrate are similar, thus suggesting that inter-tube interactions do not perturb the electronic structure on an energy scale of 77 K.

We have also characterized a number of semiconducting SWNTs in our studies. Indeed, more than half of the SWNTs observed either as isolated tubes or in ropes were found to be moderate gap semiconductors. A typical example of the atomically resolved structural and tunnelling spectroscopy data obtained from isolated SWNTs is shown in Fig. 3. Analysis of the image (Fig. 3a) shows that the upper tube has a chiral angle of $11.2 \pm 0.5°$ (that is, opposite helicity to the tubes in Fig. 2) and a diameter of 0.95 ± 0.05 nm. These angle/diameter constraints agree best with the 11.7°/1.0 nm for a (14,–3) tube, although the 10.9°/1.08 nm angle/diameter of the next closest (15,–3) indices are close to our uncertainty. The I–V data recorded with this atomic-resolution image (Fig. 3b inset) shows distinctly different behaviour from the metallic tubes and is consistent with a semiconductor; that is, the current is very small for $-300 \leqslant V \leqslant +400$ mV but increases sharply when $|V|$ is increased further. The calculated $(V/I)\mathrm{d}I/\mathrm{d}V$ shows sharp increases at −325 and +425 mV that correspond to the conduction and valence band edges in the LDOS, and thus we assign a bandgap of 750 meV.

The observed semiconducting behaviour is consistent with the expectation that a (14,–3) tube should be a moderate gap semiconductor (that is, $(2n + m)/3$ is not an integer). In addition, we have observed similar semiconducting behaviour for other chiral and zigzag tubes characterized with atomic resolution. A summary of the energy gaps (E_g) obtained from these measurements for tubes with diameters between 0.6 and 1.1 nm is shown in Fig. 3c. These results show the expected[1] 1/diameter (d) dependence, and can be fitted to $E_g = 2\gamma_0 a_{C-C}/d$, where $\gamma_0 = 2.45$ eV is the nearest-neighbour overlap integral and a_{C-C} is the C–C distance. Significantly, this value of γ_0 is in good agreement with the value (2.5 eV) determined from calculations[1], and provides an additional consistency check in this work.

Our observation of semiconducting and metallic SWNTs with subtle changes in structure clearly confirm the remarkable electronic behaviour of the nanotubes that may be exploited in future

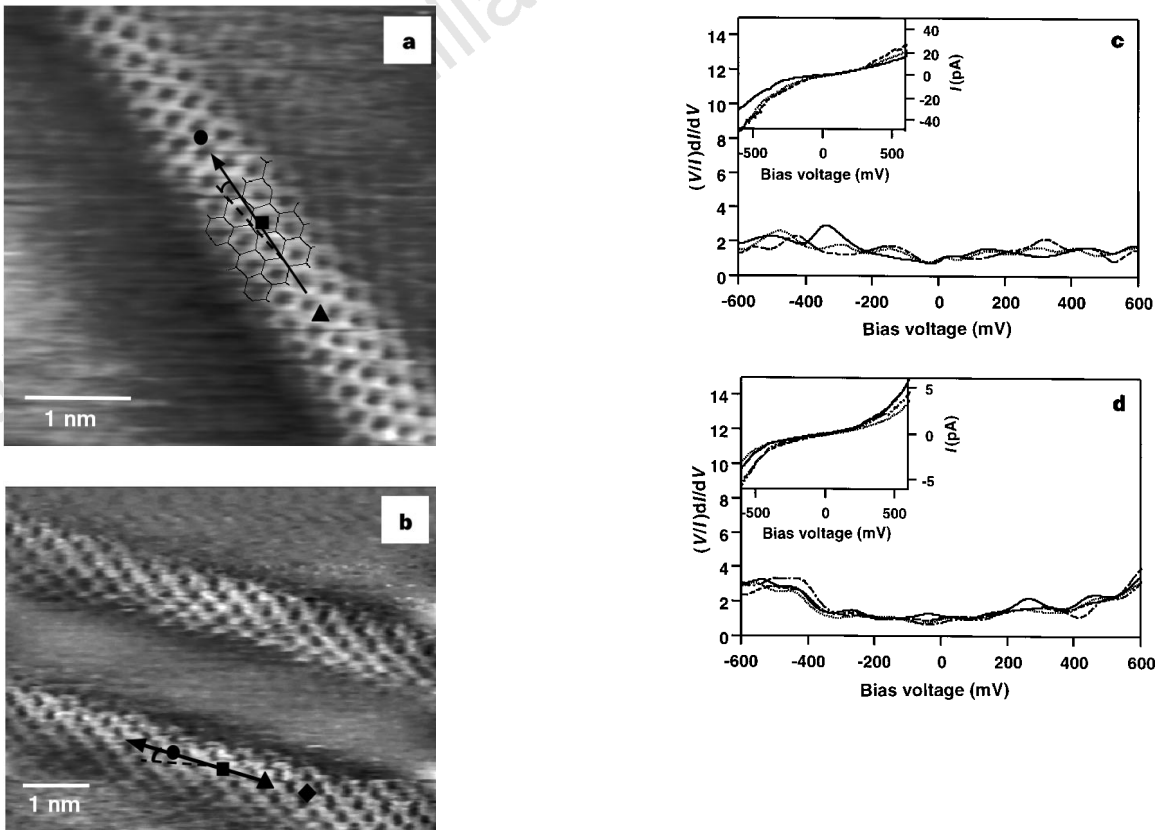

Figure 2 Atomic structure and spectroscopy of metallic SWNTs. STM images of **a**, a SWNT exposed at the surface of a rope and **b**, isolated SWNTs on a Au(111) substrate. The images were recorded in the constant-current mode with bias voltages of 50 and 150 mV, respectively, and tunnelling current of 150 pA. The images were low-pass filtered. The tube axes in both images are indicated with solid, black arrows, and the zigzag direction are highlighted by dashed lines. A portion of a two-dimensional graphene layer is overlaid in **a** to highlight the atomic structure. The symbols in **a** and **b** correspond to the locations where I–V were measured. The two parallel tubes in **b** could correspond to distinct tubes or to an image of one tube by two tips, although the interpretation of our results is not affected by either explanation. **c**, **d**, Calculated normalized conductance, $(V/I)\mathrm{d}I/\mathrm{d}V$, and measured I–V (inset) from the locations indicated in **a**, **b**: —/●; ···/■; - - -/▲; ···/◆. The feature at –400 mV in **d** was not observed for every metallic tube, and may arise from a nanotube–substrate interaction.

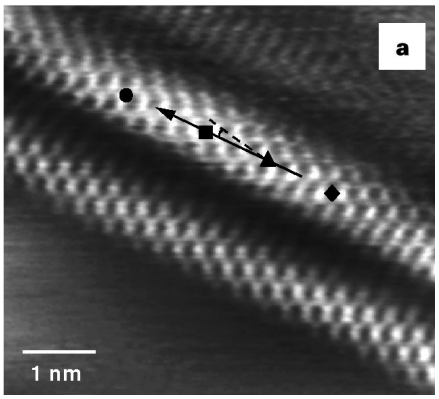

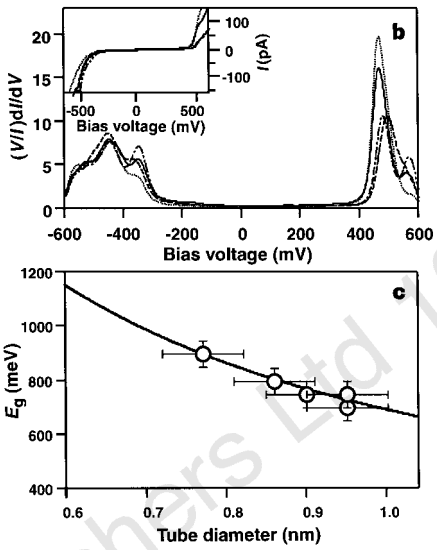

Figure 3 Structure and spectroscopy of semiconducting SWNTs. **a**, Constant current image of isolated SWNTs on a Au(111) surface recorded with a bias voltage of 300 mV and a tunnelling current of 150 pA. The solid, black arrow highlights the tube axis, and the dashed line indicates the zigzag direction. **b**, Calculated normalized conductance and measured *I*–*V* (inset) data from the positions indicated by the symbols in **a**; the symbols are the same as in Fig. 2. **c**, Summary of energy gap (E_g) versus tube diameter data obtained in these studies. The angles/diameters of these points may be fitted with (10,0), (11,0), (11,0), (14,–3) and (13,–1). The solid line corresponds to the fit described in the text.

applications. We believe that these results also have significant implications for the present. First, the data show a richness of structures (and electronic properties), and indicate that no one SWNT type dominates. This observation contrasts with previous suggestions[11,15] that SWNTs prepared by laser vaporization consist primarily of (10,10) armchair tubes. Because our STM measurements are biased towards SWNTs that have separated from the outer portion of ropes, it is possible that this discrepancy reflects a rope structure in which (10,10) armchair tubes lie at the core and are surrounded by structurally diverse tubes. We believe that it will be possible to test this idea by cutting and etching the ropes (J. Liu, R. E. Smalley, T.W.O., J.L.H., P.K. and C.M.L., work in progress); such results could help to elucidate the growth mechanism.

The presence of a large fraction of semiconducting nanotubes should be considered when interpreting electrical measurements that probe the bulk properties of ropes, such as the temperature-dependent resistivity[16] and doping-induced changes in electrical conductivity[17]. For example, the cross-over in resistivity with temperature[16] could have a trivial explanation in terms of variable-range hopping between metallic tubes separated by semiconducting tubes. We believe that STM characterization combined with growth and purification studies will provide a rational pathway for producing structurally homogeneous samples of nanotubes in the future. □

Methods

SWNT samples were prepared by laser vaporization[11], and deposited by spin-coating organic suspensions onto Au(111) surfaces. Immediately after deposition, the substrate was loaded into an ultra-high vacuum (UHV) chamber and transferred under vacuum to the UHV STM that was stabilized at 77 K. Atomic force microscopy and field-emission scanning electron microscopy showed that the samples consisted primarily of SWNT ropes spaced ~10 μm apart. Imaging and spectroscopy measurements were made using etched tungsten tips with the bias (V) applied to the tip. The resolution and calibration of the STM were confirmed *in situ* by imaging the Au(111) atomic lattice and steps. The nanotube diameters were determined by deconvolution of the tip radius from the observed images; typically, 400 cross-sections were averaged and used in the deconvolution. The parameters obtained from this model were reasonable and in agreement with those obtained from Au steps in the same experiments.

Spectroscopy measurements were made by recording and averaging 5–10 *I*–*V* curves at specific locations on atomically resolved SWNTs. Typically, 6–8 distinct locations were measured for a given atomic image. To ensure the reliability of these measurements we routinely checked that clean areas of the Au(111) substrate showed typical metallic *I*–*V* behaviour and the expected two-dimensional surface state[14], and that I varied exponentially with tip–sample separation. The normalized conductance $(V/I)\mathrm{d}I/\mathrm{d}V$ was calculated from digital *I*–*V* data using standard methods[13].

Received 10 October; accepted 26 November 1997.

1. Dresselhaus, M. S., Dresselhaus, G. & Eklund, P. C. *Science of Fullerenes and Carbon Nanotubes* (Academic, San Diego, 1996).
2. Mintmire, J. W., Dunlap, B. I. & White, C. T. Are fullerene tubes metallic? *Phys. Rev. Lett.* **68,** 631–634 (1992).
3. Hamada, N., Sawada, S. & Oshiyama, A. New one-dimensional conductors: graphitic microtubules. *Phys. Rev. Lett.* **68,** 1579–1581 (1992).
4. Saito, R., Fujita, M., Dresselhaus, G. & Dresselhaus, M. S. Electronic structure of chiral graphene tubules. *Appl. Phys. Lett.* **60,** 2204–2206 (1992).
5. Saito, R., Fujita, M., Dresselhaus, G. & Dresselhaus, M. S. Electronic structure of graphene tubules based on C_{60}. *Phys. Rev. B* **46,** 1804–1811 (1992).
6. Zhang, Z. & Lieber, C. M. Nanotube structure and electronic properties probed by STM. *Appl. Phys. Lett.* **62,** 2972–2974 (1993).
7. Olk, C. H. & Heremans, J. P. Scanning tunneling spectroscopy of carbon nanotubes. *J. Mater. Res.* **9,** 259–262 (1994).
8. Ge, M. & Sattler, K. Vapor-condensation generation and STM analysis of fullerene tubes. *Science* **260,** 515–518 (1993).
9. Carroll, D. L. *et al.* Electronic structure and localized states at carbon nanotube tips. *Phys. Rev. Lett.* **78,** 2811–2814 (1997).
10. Ge, M. & Sattler, K. STM of single-shell nanotubes of carbon. *Appl. Phys. Lett.* **65,** 2284–2286 (1994).
11. Thess, A. *et al.* Crystalline ropes of metallic carbon nanotubes. *Science* **273,** 483–487 (1996).
12. Journet, C. *et al.* Large-scale production of single-walled carbon nanotubes by the electric-arc technique. *Nature* **388,** 756–758 (1997).
13. Stroscio, J. A. & Feenstra, R. M. in *Scanning Tunneling Microscopy* (eds Stroscio, J. A. & Kaiser, W. J.) 95–141 (Academic, New York, 1993).
14. Everson, M. P., Jaklevic, R. C. & Shen, W. Measurement of the local density of states on a metal surface: Scanning tunneling spectroscopic imaging of Au(111). *J. Vac. Sci. Technol. A* **8,** 3662–3665 (1990).
15. Rao, A. M. *et al.* Diameter-selective Raman scattering from vibrational modes in carbon nanotubes. *Science* **275,** 187–191 (1997).
16. Fischer, J. E. *et al.* Metallic resistivity in crystalline ropes of single-wall carbon nanotubes. *Phys. Rev. B* **55,** 4921–4924 (1997).
17. Lee, R. S., Kim, H. J., Fischer, J. E., Thess, A. & Smalley, R. E. Conductivity enhancement in single-walled carbon nanotube bundles doped with K and Br. *Nature* **388,** 255–257 (1997).

Acknowledgements. We thank J. Liu and R. E. Smalley for discussions and samples, and D. Vezenov for help with the Au deposition. T.W.O. acknowledges fellowship support from the US NSF. This work was supported by the NSF Division of Materials Research.

Correspondence and requests for materials should be addressed to C.M.L. (e-mail:cml@cmliris.harvard.edu).